Molecular dynamics simulations of liquid crystal molecules on a polyimide monolayer

Makoto Yoneya[a]; Yasushi Iwakabe[ab]

[a] Hitachi Research Laboratory, Hitachi, Ltd., Hitachi, Ibaraki, Japan [b] Electron Tube & Devices Div., Hitachi Ltd., Chiba, Japan.

PLEASE SCROLL DOWN FOR ARTICLE

Molecular dynamics simulations of liquid crystal molecules on a polyimide monolayer

by MAKOTO YONEYA* and YASUSHI IWAKABE†

Hitachi Research Laboratory, Hitachi, Ltd. 7-1-1 Omika, Hitachi, Ibaraki 319-12, Japan

Preliminary results are presented on the molecular dynamics simulations of alignment of the liquid crystal molecule, 4-n-octyl-4'-cyanobiphenyl (8CB), on a polyimide (pyromelltic dianhydride-p-phenylene diamine) oligomer monolayer. We actually simulated a three-layer system, i.e., liquid crystal molecule/polyimide oligomer/a basal plane of graphite. First, simulations of the oligomers adsorbed on graphite were done in order to obtain reasonable adsorption structures, as the pre-stage simulation of the three-layer system. Then, by placing a liquid crystal layer on top, the three-layer system was simulated. The stable liquid crystal alignment direction on the polyimide monolayer was found roughly to be the polyimide chain direction with zero pretilt in this combination of liquid crystal and polymer materials. The calculated adsorption energy of an 8CB molecule to the polyimide monolayer was 128 kJ mol^{-1} and the carbonyl group of the polyimide was the main adsorption site.

1. Introduction

The alignment mechanism of liquid crystal molecules at the liquid crystal/substrate interface in a liquid crystal display (LCD) has recently attracted considerable attention. An LCD consists of two glass substrates sealed together with a liquid crystal-filled gap between them of a few microns. The inner surfaces of the glass substrates are coated with polymer (generally polyimide) layers which provide a uniform alignment of the liquid crystal molecules [1]. It is becoming more and more important to understand the alignment mechanism at this liquid crystal/polymer layer interface because the alignment condition of the interface greatly affects display imaging quality, especially in the latest large area displays. However, the mechanism has not yet been clarified since analytical methods with molecular or even atomic level resolution are essentially required for the clarification.

Recently, direct observations of the liquid crystal molecules on inorganic substrates (for example, graphite [2] or MoS$_2$ [3]) have become possible using scanning tunnelling microscopy (STM). Yet another new approach with atomic level resolution is application of molecular simulations like molecular dynamics (MD) or Monte Carlo methods. Ikeda et al. [4], Yoneya and Iwakabe [5] and Cleaver et al. [6], performed MD simulations of the liquid crystal molecule 4-n-octyl-4'-

cyanobiphenyl (8CB) on a basal plane of graphite, corresponding to the above mentioned STM observations. These experimental or simulation studies of a rather simple (i.e. liquid crystal/graphite) interface are a good starting point for further investigation of the actual interface in an LCD. However, the actual interface of an LCD is not merely a liquid crystal/polymer interface. The alignment polymer layers are treated with a rubbing process in LCD mass production. The rubbing process is a mechanical treatment, during which, the polymer layer is rubbed with a polymer cloth. This process effectively produces a liquid crystal molecule alignment in the rubbing direction. Although the rubbing process was discovered in 1911 [7], it still is not fully understood. Several hypotheses have been proposed to explain its mechanism. For example, one is that microgrooves which are generated during the rubbing produce the alignment by macroscopic elastic effects [8]. Another is that the polymer chains near the rubbed surface are re-oriented in the rubbing directions and then these aligned chains serve as an anisotropic template for liquid crystal alignment [9]. Both of these are currently considered as the main effects of the rubbing process.

In this study, we present results of molecular dynamics simulations of the liquid crystal molecule alignment on a polyimide monolayer. A three-layer system was simulated, i.e. liquid crystal molecule/polyimide oligomer/ a basal plane of graphite. The interface of the liquid crystal/polyimide monolayer is considered to be

* Author for correspondence.
† Current address: Electron Tube & Devices Div., Hitachi Ltd., 3300 Hayano, Mobara, Chiba 297, Japan.

a simplified model for the actual interface in an LCD. Our reasons for inclusion of the graphite surface in the system are twofold. The first is that we wanted to compare our simulation results with corresponding STM observations. Graphite is a standard substrate for STM observations due to its conducting properties and the ease with which a clean cleaved surface can be obtained. Secondly, we needed a polyimide surface structure before studying the alignment of liquid crystal molecules on it. For this model surface, the adsorption structures of polyimide on graphite would be a good choice since they have been studied by STM [10] and AFM [11]. Fujiwara et al. [10], also performed a MD simulation and compared the results with those of their STM study. Actually, we first did an MD simulation of the polyimide oligomers adsorbed on graphite as a pre-stage simulation of the three-layer system to obtain a reasonable oligomer adsorption structure on graphite. We considered the adsorption structure to be well aligned one and started the MD run from a perfectly aligned initial structure. This assumption seems valid since polyimide chains are considered to be well aligned at the actual LCD aligning layer due to the rubbing process as mentioned above. This means that only the chain re-orientation aspect of the rubbing process was taken into account and the rubbed polymer surface was modelized as a well-aligned surface. In this respect, our model more directly corresponds to liquid crystal alignment with drawn polymer tapes [12] or Langmuir–Blodgett films [13]. After obtaining the adsorption structure of the polyimide oligomer on graphite, the three-layer system with the interface of main interest (i.e. liquid crystal/polyimide) was simulated by placing a liquid crystal monolayer on the top.

Adsorption structures of polyimide oligomers on graphite, and liquid crystal molecules on the polyimide oligomers are calculated. We also examined the energetics of the adsorbed structures and the adsorption portions onto graphite or the polyimide monolayer.

2. Simulation model

The simulated liquid crystal molecule and polyimide oligomer were 4-n-octyl-4'-cyanobiphenyl (8CB, see figure 1(a)) and three repeating units of pyromelltic dyanhydride-p-phenylene diamine (PMDA-PPD, see figure 1(b)), respectively. PMDA-PPD was selected for its relative rigidity as compared to other polyimides, so it is expected to have a simple linear alignment and a short relaxation time. Both the molecular models for 8CB and PMDA-PPD were detailed atomic models, except for the CH_2 and CH_3 groups, which were regarded as united atoms. The ends of the oligomer chains were terminated by united CH_3 atoms.
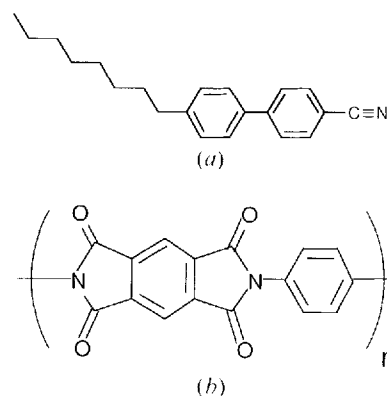

Figure 1. Chemical structures of (a) 8CB and (b) PMDA-PPD.

The following GROMOS force field [14] was used for inter- and intramolecular interaction potentials.

$$U_{total} = \sum_{atomic\ pairs} \left(\frac{A_{ij}}{r_{ij}^{12}} - \frac{B_{ij}}{r_{ij}^{6}} + \frac{q_i q_j}{4\pi\varepsilon_0 r_{ij}} \right)$$
$$+ \sum_{bonds} \frac{k_d}{2} (d - d_0)^2 + \sum_{angles} \frac{k_\theta}{2} (\theta - \theta_0)^2$$
$$+ \sum_{imp.dih.s} \frac{k_\psi}{2} (\psi - \psi_0)^2$$
$$+ \sum_{dihedrals} k_\phi (1 + \cos(n\phi - \delta)) \tag{1}$$

The first term represents the non-bonding interaction due to the Lennard–Jones and Coulomb potentials. The remaining terms correspond to bond stretching, bond angle bending, and improper (out of plane) and proper dihedral angle torsioning potential, respectively. Basically, force field parameters were taken from GROMOS force field parameters. The parameters specific to 8CB and the partial atomic charge distribution of the 8CB molecules were taken from those of Picken et al. [15], hence our 8CB model was the same as that for the 5CB (4-n-pentyl-4'-cyanobiphenyl) molecule used by Picken et al., except for its side chain length. The parameter values specific to polyimide were set after referring to the literature [16,17] and so as not to contradict other GROMOS parameters. The values are listed in appendix 1. Partial atomic charges of the oligomer were obtained by an extended-Hückel molecular orbital method and are listed in appendix 2. The (spherical) cut-off length of the non-bonding interactions was set to 1·8 nm.

The graphite surface model we used was the same as in Yoneya and Iwakabe [18]. It was originally derived by Taji et al. [19], for MD simulations of interstitial atoms in graphite. Only van der Waals (in the Lennard–

Jones form) and no electrostatic (i.e. image charge) interactions were included between the graphite surface and the oligomer and liquid crystal molecules. In the case of a surface simulation, the ideally structured rigid graphite model has often been used to minimize computational efforts [20]. However, here we used the flexible graphite model since we considered temperature of the graphite surface was an important factor in discussing the thermodynamic stabilities of adsorbed structures [18]. The basal plane of the graphite was located on the *x–y* plane, and we applied a two-dimensional periodic boundary condition (to the whole system) in this plane to avoid unfavourable edge effects. The actual size of the periodically repeated section of the graphite plane was 4.26×3.69 nm.

3. Polyimide oligomers on graphite

3.1. *Simulation set-up*

First, we have to set the initial structures to start the MD run for the polyimide oligomers on graphite. As stated in the introduction, the STM and MD simulation studies of a polyimide (pyromelltic dianhydride-*p*-oxydianiline, PMDA-ODA) on graphite by Fujiwara *et al.* [10], give some hints for it. Thus, adjacent chain spacing of the polyimide oligomers and their imide ring direction were set to about 0·8 nm and parallel to the graphite surface, respectively, by referring to the MD results. In contrast with PMDA-ODA, PMDA-PPD in our study is expected to have a linear conformation and alignment structure. Then, the alignment direction of PMDA-PPD chains on graphite surface must reasonably be determined in the initial structure. To determine this direction, we calculated the static energy of a system with a graphite surface and one PMDA-PPD monomer on it while varying its relative orientations to the graphite surface. The calculation was done without the two-dimensional periodic boundary condition or any molecular deformation. The average distance between the PMDA-PPD monomer and the graphite surface was set to 0·4 nm. Figure 2 shows the resultant dependence of the adsorption interaction energy (U_{int}) on the long axis orientations (ϕ) of the PMDA-PPD monomer to the $\langle 2\bar{1}\bar{1}0 \rangle$ direction of graphite surface. No clear adsorption selectivity in the relative orientations was obtained, within an energy difference of 0·07 kJ mol^{-1}. In the same kind of plot for the 8CB molecule, we obtained clear selectivity with an energy difference of 1·6 kJ mol^{-1} [5]. From these results, we arbitrarily selected the chain direction of $\langle 2\bar{1}\bar{1}0 \rangle$ in the graphite surface in the initial structures. Figure 3 (*a*) shows the initial structure.

Starting from this structure, we did 100 steps of energy minimization and then, 400 steps of initial relaxation dynamics with the Boltzmann distributed initial velocit-
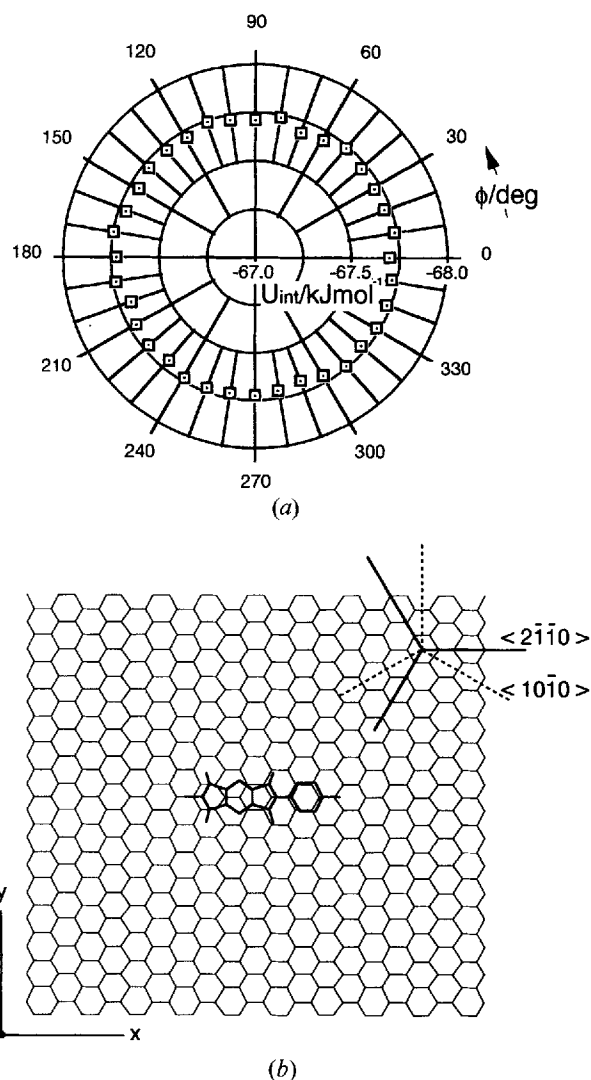

Figure 2. (*a*) Dependence of interaction energy (U_{int}) on the angle (ϕ) between the long axis of the PMDA-PPD monomer and the surface orientation of the graphite. (*b*) The configuration corresponding to the 0° angle case in (*a*).

ies of atoms. Production runs were then done with a time-integration step of 0·5 fs up to 30 ps (corresponding to 60 000 simulation steps). During these runs, the temperature of the system was maintained around 300 K by using weak coupling to a heat bath [21].

3.2. *Results*

In figure 3 (*b*), we show the instantaneous structure after 30 ps in the simulation starting from the initial structure in figure 3 (*a*). From this figure, oligomer chain spacings were packed from the initially set distance (0·8 nm) and oligomer rings were declined to the graphite surface. Chain orientation of the surface was not
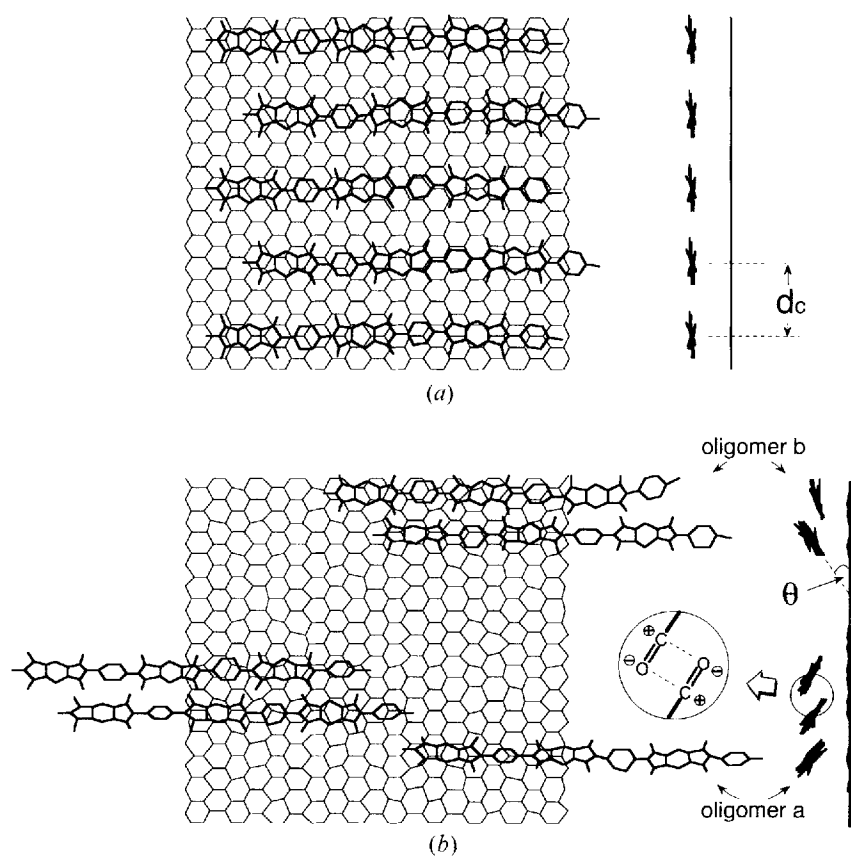
(a)

oligomer b

θ

oligomer a

(b)

Figure 3.   (a) Initial and (b) instant-
aneous structures after a 30 ps
MD run of a five-oligomer
system. Here, d_c and θ stand
for the adjacent chain spacing
and the oligomer ring declina-
tion angle to the graphite
surface, respectively.

changed. In figure 4, time-evolutions of adjacent chain separations d_c and declination angles θ (see figure 3(b) for their definitions) of oligomers to the graphite surface are plotted. Here, the chain separation and the declination angles were actually calculated as the y direction distance of the oligomer centers of masses and the angles of the second longest principle inertial axis of the oligomer to the x–y plane, respectively. In these time-evolution graphs, chain separations were quickly packed to an average values of 0·46 nm, and oligomers were declined to an average declination angle of 37° except for oligomer a and b in figure 3(b). The packing and ring declination were caused by strong dipole interactions between carbonyl groups of the imide rings as illustrated in figure 3(b). And the two oligomers, a and b were relatively less declined and fluctuations in the declination angles were at an edge position without an adjacent oligomer for coupling. The adjacent chain spacing after the packing (i.e., 0·46 nm) was close to the observed value (about 0·5 nm for PMDA-ODA on graphite) which Fujiwara et al. [10], obtained by STM. And they also suggested molecular declination relative to the graphite surface judging from the molecular size and the adjacent chain separation.

Next, we did a simulation to check the stabilities of the resultant structure obtained above. The initial structure was set with a chain separation of 0·46 nm and declination angle of 37° for eight oligomers as in figure 5(a). The instantaneous structure after 30 ps is shown in figure 5(b) and in figure 6, we show time-evolution plots like those of figure 4. The chain separation and declination angle were kept around their initial values and the basic structure was stable. However, with a longer time-scale, the oligomer layer drifted (about 1 nm in $-y$ direction) on the graphite surface while keeping the chain separation as in figure 7. During this drift, the total energy of the system was decreased about 80 kJ mol^{-1} per oligomer. Hence the drift led to a more stable relative position between the oligomer layer and the graphite surface than that of the initial structure.

Thus, we considered that the surface structure with the obtained chain separation and declination angle would be one of the stable structures of this system. The average (over 30–32 ps) adsorption structure is shown in figure 8. We estimated adsorption energy of the oligomer onto graphite using the average energy difference between the adsorbed structure in figure 8 and the separate system of the oligomers and graphite and
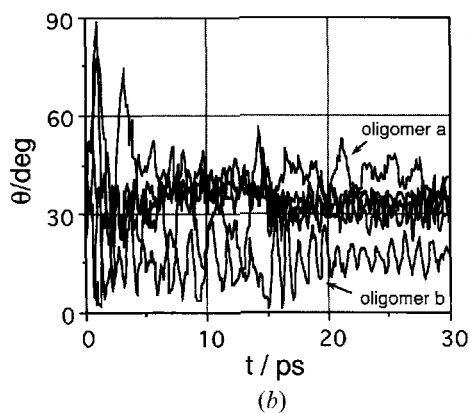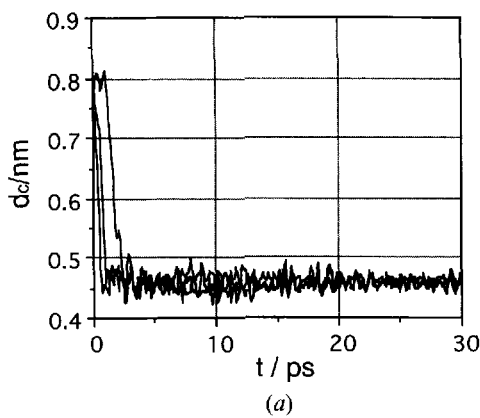
Figure 4. Evolution over time of (*a*) adjacent chain spacings d_c and (*b*) ring declination angle (θ).
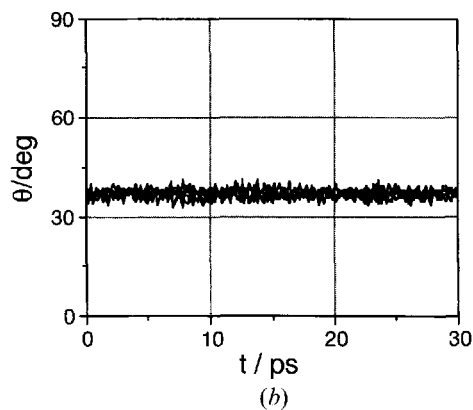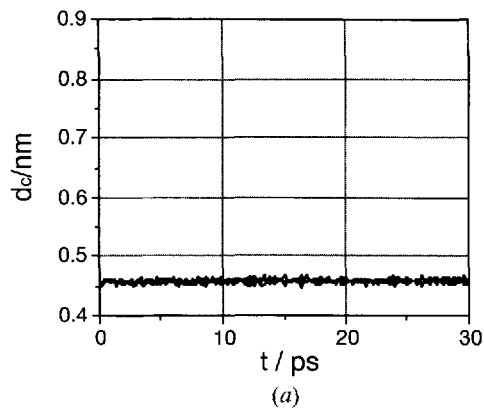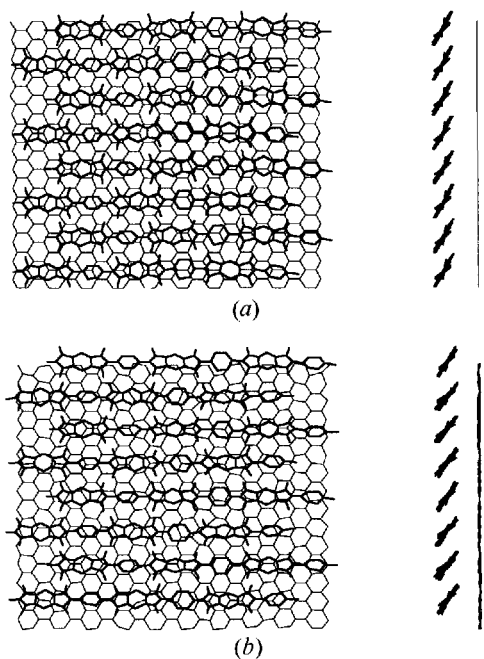

Figure 5. (*a*) Initial and (*b*) instantaneous structures after a 30 ps MD run of an eight-oligomer system.
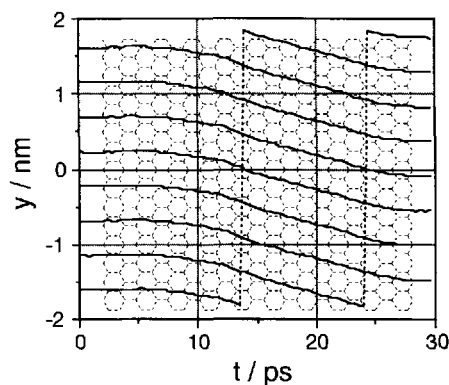

Figure 6. Evolution over time of (*a*) adjacent chain spacings d_c and (*b*) ring declination angle (θ).

Figure 7. Evolution over time of *y*-coordinate values of the oligomer centre of the mass.

obtained the value of $196 \, \text{kJ} \, \text{mol}^{-1}$. We also examined the averaged interaction energies between the oligomer atoms and the graphite surface to evaluate which part of the oligomer is the adsorption portion onto the graphite. The result is shown in figure 9. The interaction energies were all negative (stabilizing the adsorbed structure) and among them, the carbonyl groups stuck out
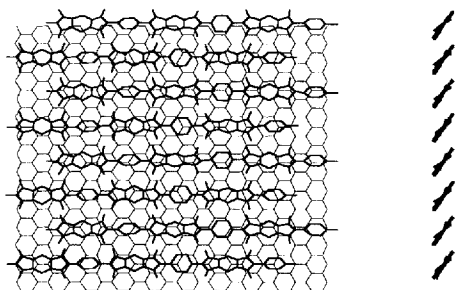
Figure 8.   Averaged structure over 30–32 ps.

to the graphite surface was larger than for other parts, i.e., these groups were considered to be the main adsorption portion.

Polyimide surface structure which obtained above is characterized by strong dipole coupling between adjacent polymer chains. And this dipole coupling causes declination of polyimide rings relative to the graphite surface in our simulations. As it mentioned in above, Fujiwara *et al.* [10], suggested molecular declination relative to the graphite surface from their STM observation of the similar polyimide. This correspondence indicated that the dipole coupling network found in our simulation will actually exist in some polymer surface as a hydrogen bonding network in the case of polyamide [22, 18]. However, the dipole coupling network in the surface structure is not observed in the other polymers with dipole moments (as in carbonyl group), like poly(ε-caprolactone). Actually, the STM images of poly(ε-caprolactone) on graphite obtained with PIE

process [23] are not successfully interpreted into a reasonable surface structure. These are also challenging subjects for the molecular simulation approach to surface science.

4.   8CB molecules on a polyimide monolayer

4.1.   Simulation set-up

Next, we did simulations of the three-layered system by adding a liquid crystal layer onto the polyimide oligomer layer which was obtained in the previous section. The structure of the 8CB liquid crystal layer was the same structure as the initial structure in the simulation of 8CB on graphite [5]. This liquid crystal monolayer consisted of ten 8CB molecules with an adjacent separation of 7·4 nm. We tried two initial structures which differed in the relative orientation of the liquid crystal molecule and oligomer chain direction. These two initial structures are shown in figures 10(a) and 10(b) and hereinafter, designated as A and B, respectively. In structure A, the 8CB biphenyl axes are oriented in the oligomer chain direction and the axes are perpendicular to the chain direction in structure B. The alignment in structure A would be the most probable with respect to Lennard–Jones interactions between chains and 8CB molecules, whereas, strong dipole interactions between cyano groups of 8CB molecules and carbonyl groups of polyimide oligomers would be expected since these terminals are nearly parallel in structure B.

Starting from these structures, and after the same initial minimization and relaxation dynamics as in the
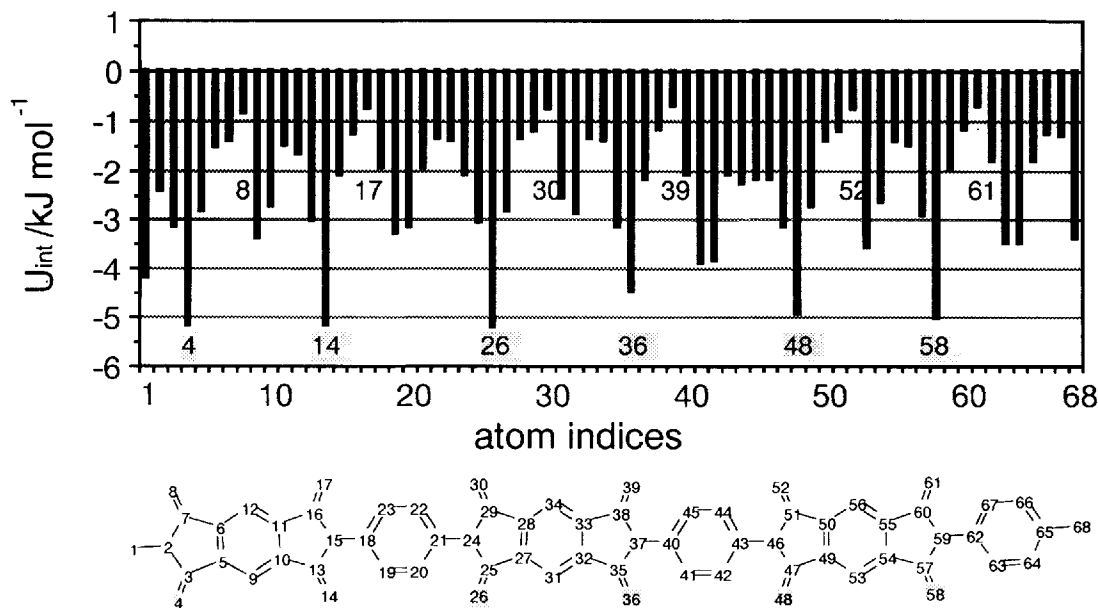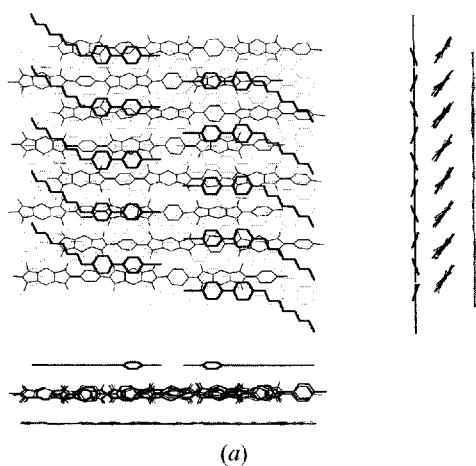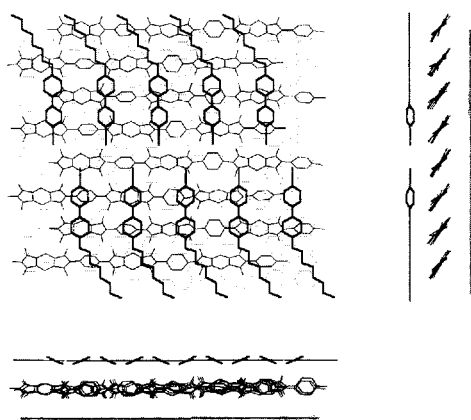

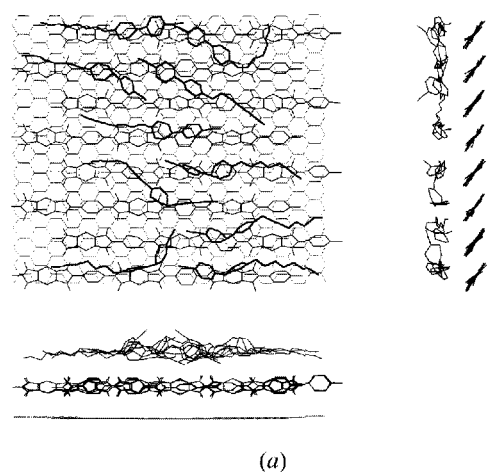Figure 9.   Atom-wise interaction energies (U_{int}) between PMDA-PPD oligomer atoms and the graphite surface.

(a)

(b)

Figure 10. Initial structures: 8CB biphenyl axes are (a) in the oligomer chain direction and (b) perpendicular to the chain direction.
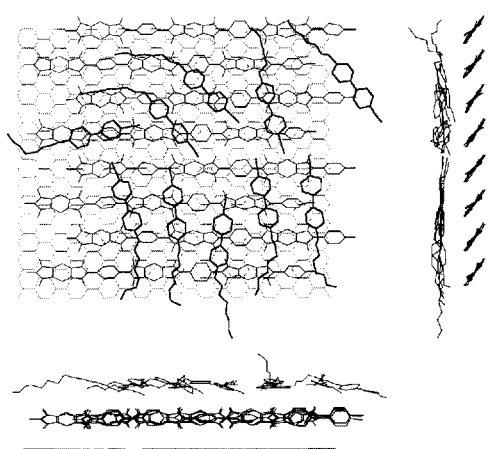

(a)

(b)

Figure 11. Averaged structures over the last 10 ps of a 500 ps MD run starting from the initial structures in (a) figure 10(a) and (b) figure 10(b).

previous section, we did production runs of up to 500 ps (corresponding to 10^6 simulation steps) with a time-integration step of 0·5 fs. The temperature of the system was maintained around 300 K as in the previous case.

4.2. Results

In figures 11(a) and 11(b), we show the averaged (in the last 10 ps) structures after 500 ps MD runs, starting from structures A and B, respectively. The order parameter and corresponding director direction of 8CB molecules were calculated by following the method described by Zannoni [24] i.e., calculate the largest positive eigenvalue and eigenvector of the order parameter tensor which is made up of molecular axis vectors. The molecular axis was determined by the principal axis of inertia of the molecule. The time-evolutions of the order parameter $\langle P_2 \rangle$ and director direction angle ϕ in the $x-y$

plane (measured from the chain direction) are shown in figures 12(a) and (b) for runs from initial structures A and B, respectively. Their corresponding director tilt out angles θ from the $x-y$ plane are shown in figures 13(a) and (b). From these figures, 8CB molecules were aligned roughly in the oligomer chain direction (within $\pm 10°$) in the resultant structure got from the initial structure A, whereas 8CB molecules were aligned with about a 70° declination from the chain in the resultant structure from structure B. Here after, these two structures are designated as structures A' and B', respectively. In the case starting from initial structure A, 8CB molecules were well aligned with an order parameter greater than 0·8 (see figure 12(a)), whereas the order parameter was decreased to less than 0·7 in the case of starting from
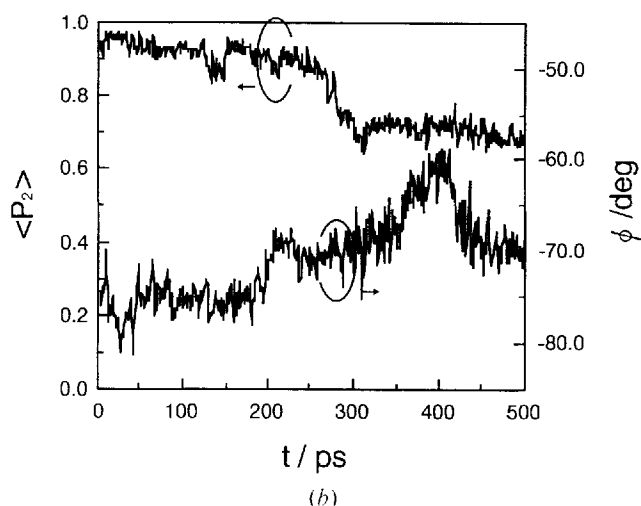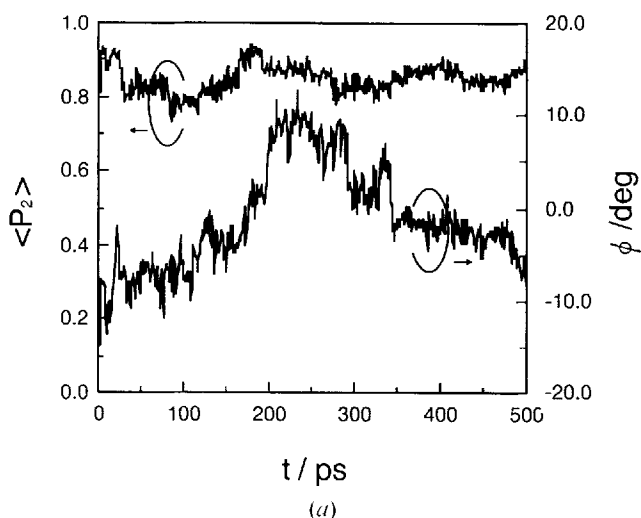
Figure 12. Evolution over time of the order parameter ($\langle P_2 \rangle$) and director angle (ϕ) in the x–y plane (measured from the oligomer chain direction) in the MD runs starting from the initial structures in (a) figure 10(a) and (b) figure 10(b).

Figure 13. Evolution over time of director tilt out of plane angle (θ) in the MD runs starting from the initial structures in (a) figure 10(a) and (b) figure 10(b).

initial structure B (figure 12(b)). This decrease was mainly caused by the 8CB molecules in the upper-half side changing their directions along with the polyimide chains as shown in figure 11(b). The director tilt out angles were very different between the runs from the initial structures A and B (see figures 13(a) and (b)). The run from structure A yielded an almost zero tilt angle (within the fluctuations of $\pm 0.4°$), whereas the tilt angle fluctuated by $\pm 3°$ in the run from structure B. However, the average tilt angle was also about zero for the latter case.

Regarding energetics, estimated adsorption energy of the 8CB molecule onto a polyimide monolayer was a little bit larger in the structure A', i.e., 128 and
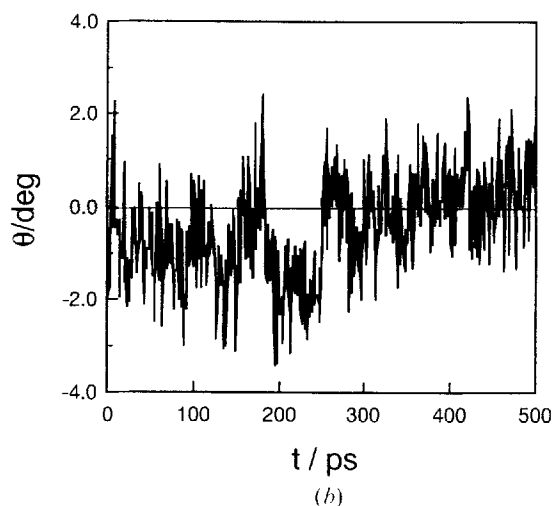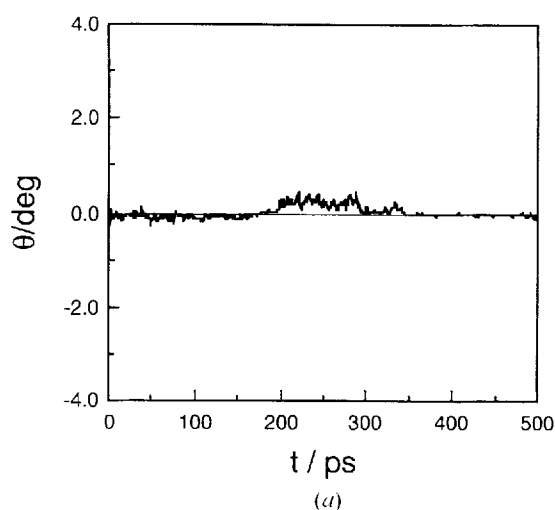
126 kJ mol^{-1} for structures A' and B', respectively. Averaged atom-wise interaction energies between the atoms in 8CB and the oligomer are shown in figures 14 and 15, corresponding to structures A' and B', respectively. In both cases, the carbonyl groups were considered to be the main adsorption site to 8CB molecules both in Coulomb and Lennard–Jones interactions. In the Lennard–Jones interaction, only the carbonyl groups in the sides which stick out into the 8CB layer acted as adsorption sites. However, the atom-wise interaction patterns differed between both cases, especially in the Lennard–Jones interaction. In structure A', the cyano group and adjacent ring of the 8CB molecule strongly interacted with the middle part of the polyimide oligomer, and the alkyl chain part of 8CB strongly interacted with the rest of the oligomer. By contrast, the
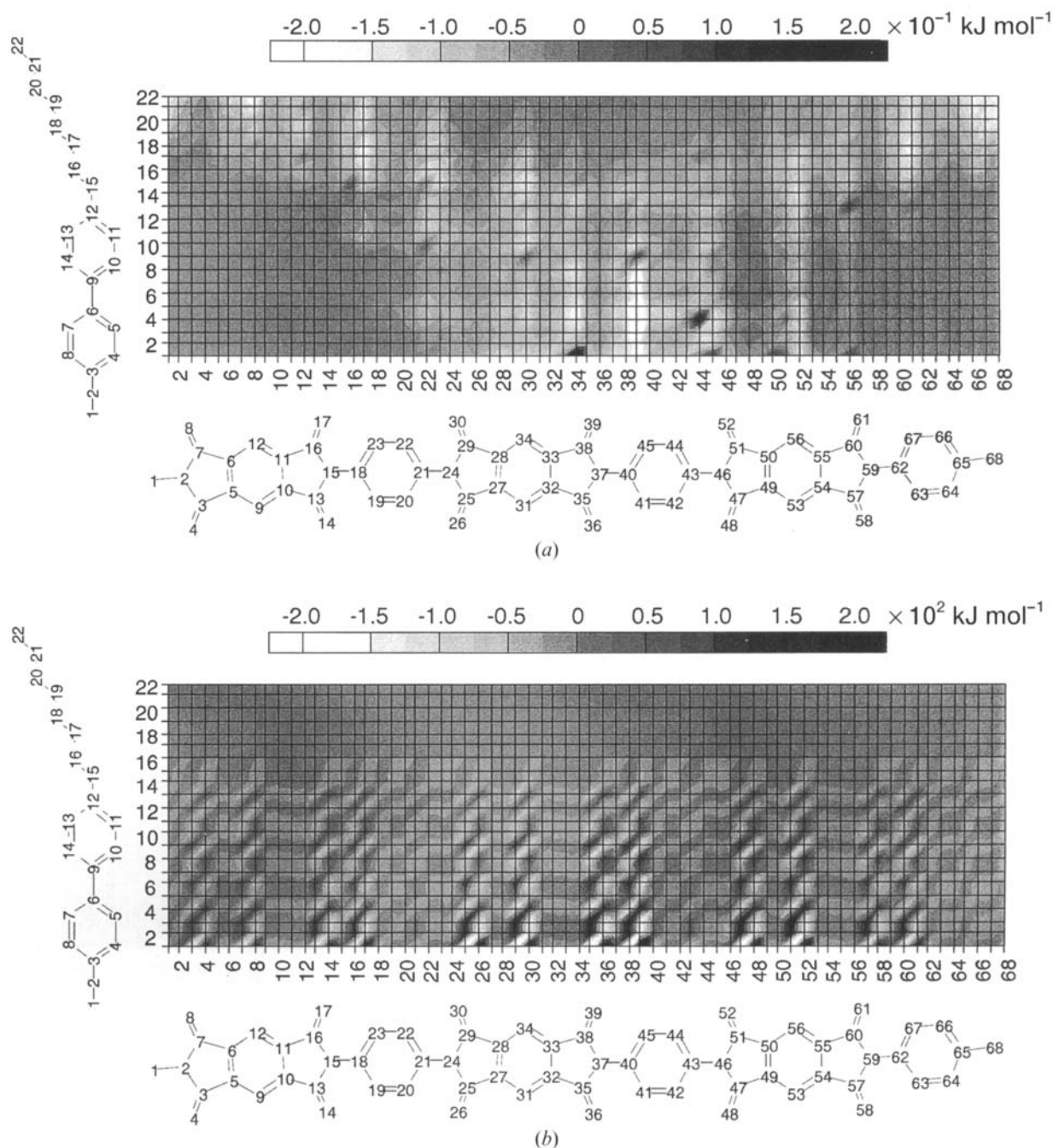
Figure 14. Atom-wise interaction energies (U_{int}) between 8CB and PMDA-PPD atoms over the last 10 ps of a 500 ps MD run starting from the initial structure in figure 10 (a).

8CB molecules interacted with about the whole part of the oligomers in structure B′. These differences directly corresponded to the structural differences between structures A′ and B′, i.e., the cyano groups of 8CB were mostly placed around the middle part of the oligomers structure A′ (see figure 10 (b)) whereas the cyano groups were distributed throughout in structure B′ (see figure 11 (b)). The Coulomb interaction is roughly 10^3 times larger than the Lennard–Jones interaction among atom-wise interactions, but overall both contributions were comparable with the ratio (Coulomb to Lennard–Jones) of 0·2 and 0·3 for structures A′ and B′, respectively. The major part of the difference (from 10^3 to 0·2 or 0·3) was the result of the fact that the major Coulomb interactions among atomic charges were dipolar pair interactions. But, the ratio of 0·2 or 0·3 is still very small with regards
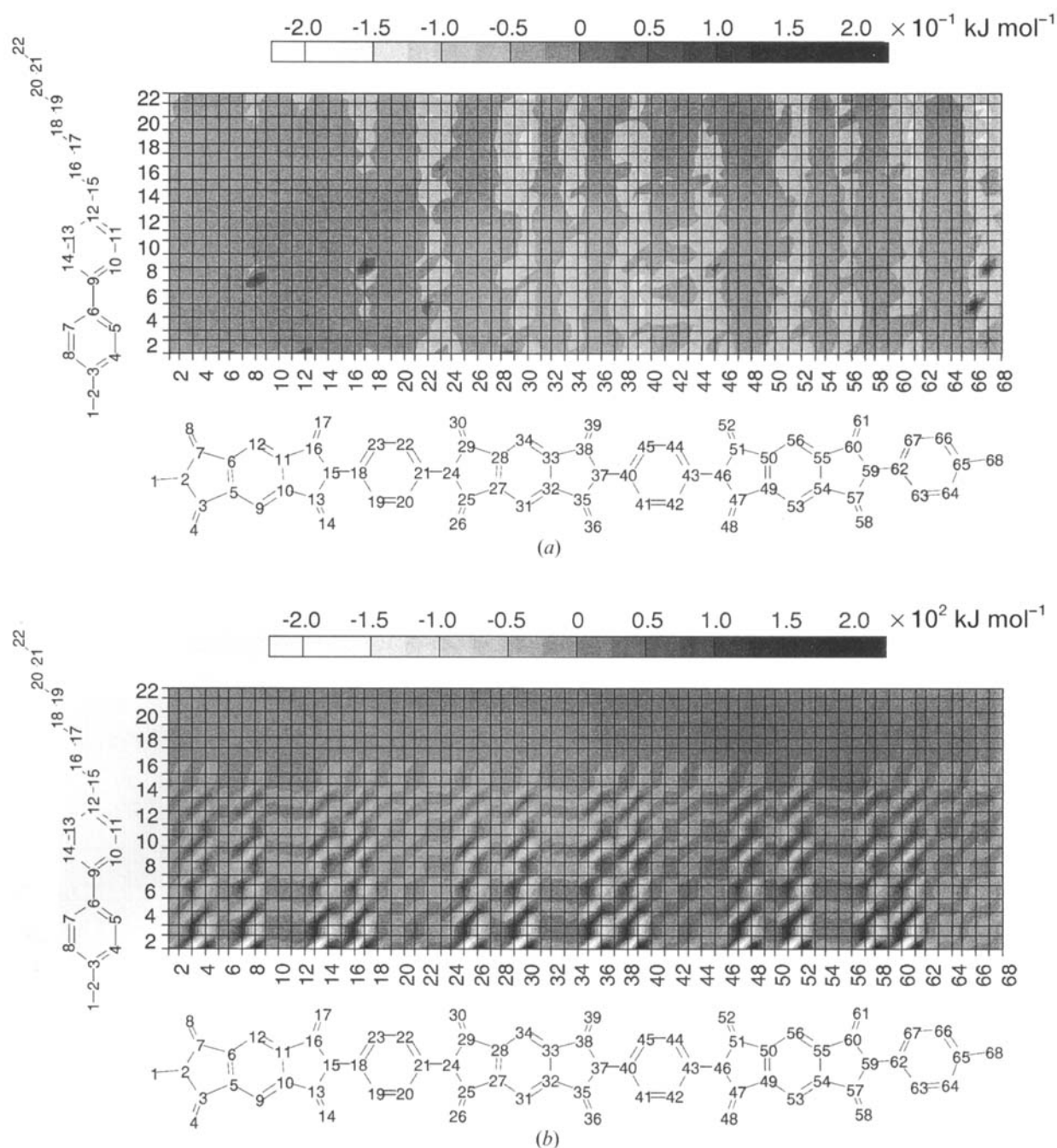
Figure 15. Atom-wise interaction energies (U_{int}) between 8CB and PMDA-PPD atoms over the last 1 ps of a 500 ps MD run starting from the initial structure in figure 10 (b).

to both the 8CB molecule and the polyimide oligomer possessing large dipoles due to their cyano and carbonyl groups, respectively.

5. Discussion

The Coulomb contribution in the intermolecular inter-action between liquid crystal molecules and oligomers is not prominent, but rather smaller than the contribu-tions of the Lennard–Jones interaction in our results. This situation was the same for both structures A′ and B′. One reason for this was in the surface (reconstructed) structure of the polyimide oligomers which we used in the calculation. The structure was characterized by strong dipole coupling between carbonyl groups of the

polyimide oligomer. As a result of this coupling, net dipole moments of these carbonyl group were not pronounced in the liquid crystal 8CB layer. To look at this, we calculated electrostatic potentials over the polyimide monolayer which was calculated in §3 as figures 3(b) and 5(b). The electrostatic potentials were calculated at mesh points in the x–y plane with the z direction distance about 0·6 nm from the oligomer layer. The results are shown in figures 16(a) and (b) and they correspond to the structures in figures 3(a) and 5(b), respectively. Large electrostatic potentials were found only in figure 16(a) and especially at the edge of the polyimide oligomer which had no adjacent oligomer to make a dipole coupling. On the other hand, the well-structured

(coupled) polyimide monolayer in figure 16(b) gave a relatively weak net electrostatic potential over the whole area. These results showed that we have to take into account not only single chain characteristics [25], but also the higher order structure of chains in some cases. These results also suggested the edge regions of the well-aligned oligomer domain play an important role in liquid crystal alignment by their strong electronic potentials.

Structure A′ with 8CB molecules aligned roughly along the polyimide chain direction (see figure 11(a)) had a slightly larger adsorption energy than structure B′ with the 8CB molecules aligned roughly perpendicular to the chain (see figure 11(b)). Furthermore, the 8CB
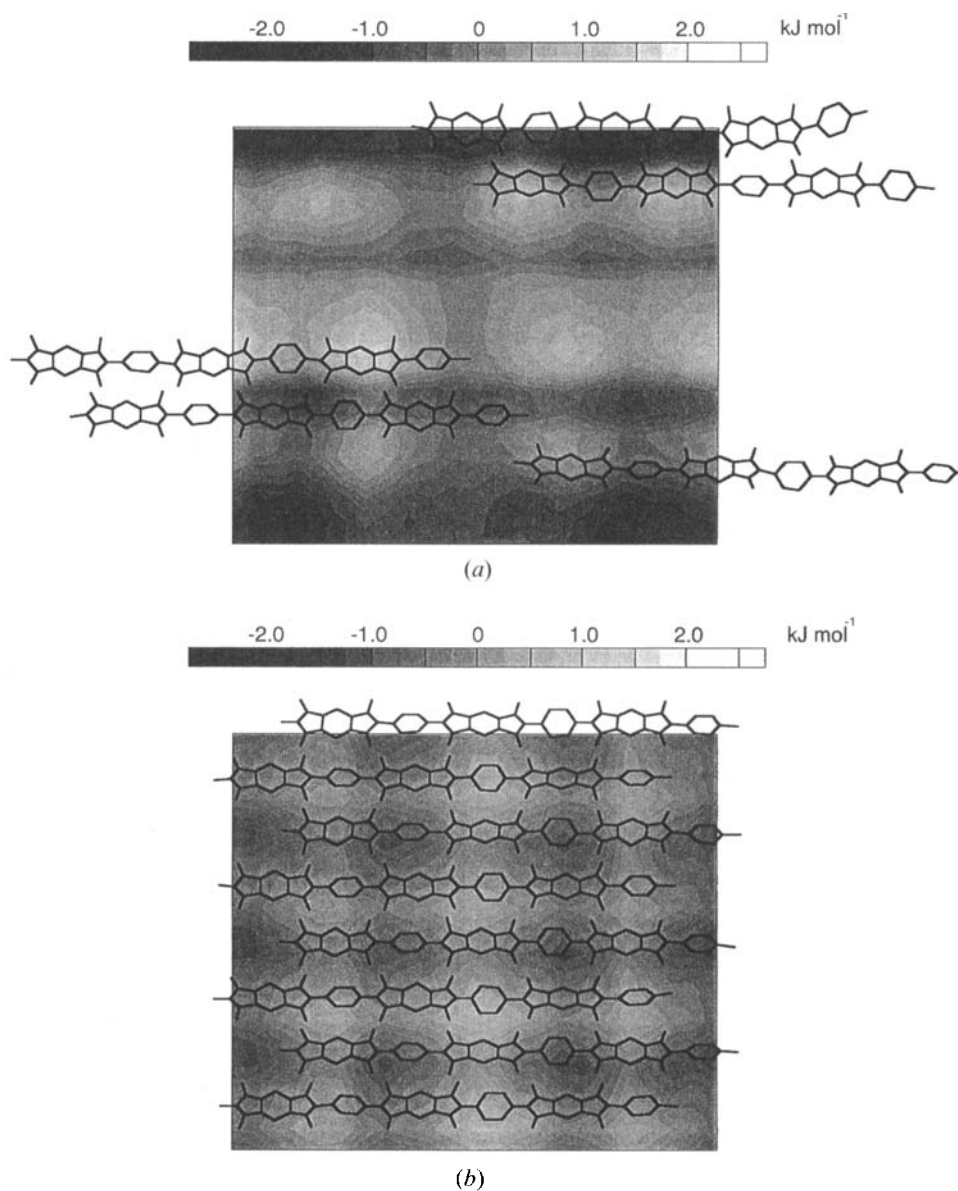

Figure 16. Electrostatic potentials over the oligomer layer structures in (a) figure 3(b) and (b) figure 5(b).

molecules, especially in the upper-half side, were tending to align with the polyimide chain direction in the run from figure 11 (b). Thus, the former structure would be the more probable alignment structure from our simulation results. As mentioned in the introduction, our model system more directly corresponds to the liquid crystal alignment by Langmuir–Blodgett (LB) films than that by the rubbing process. Murata et al. [13], reported liquid crystal alignment using the LB film of the same polyimide as ours. They obtained good liquid crystal alignment ($\langle P_2 \rangle \sim 0.73$) in the direction of the polyimide chains which were oriented by lifting a substrate in the LB film formation process. Furthermore an almost zero pretilting of the liquid crystal molecules was observed when the LB film was treated high (250°C) temperature to achieve a high imidization ratio. Our simulation results of the alignment direction and the small pretilting were in good correspondence with these experimental results.

So far, the alignment by LB films has resulted in much smaller pretilting than by the rubbing process and so do the simulations. If we succeed in reproducing high pretilting with other polymers or by adding another element which was not taken into account in this study, the polymer difference or the element will be related to the pretilting mechanism in either the rubbing or non-rubbing process. We believe molecular simulation will be a powerful tool, especially for identifying atomic level interactions which are related to the liquid crystal alignment and pretilting mechanism.

Appendix 1.   Potential parameters of the polyimide oligomer

Table A 1.1.
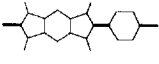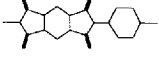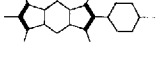
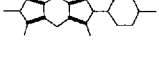| Bond type	k_d/Mj mol nm^{-2}	d_0/nm
(structure)	418.6	0.1350
(structure)	502.3	0.1230
(structure)	418.6	0.1330
(structure)	418.6	0.1421
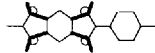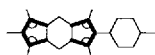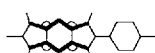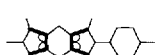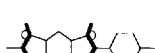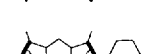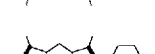
Table A 1.2.

Bend type	k_θ/kJ mol rad^{-2}	θ_0/deg
(structure)	418.6	128.5
(structure)	418.6	103.5
(structure)	418.6	132.0
(structure)	418.6	108.0
(structure)	418.6	128.0
(structure)	418.6	117.0
(structure)	418.6	121.5

Table A 1.3.
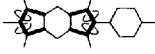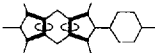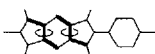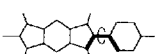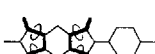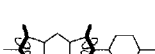
Improper type	k_ϕ/kJ mol^{-1} rad^{-2}	ϕ_0/deg
(structure)	167.4	0.0
(structure)	167.4	0.0

Table A 1.4.

Torsion type	k_ϕ/kJ mol	δ/deg	n
(structure)	41.86	180.0	2
(structure)	502.3	0.0	10
(structure)	41.86	180.0	2
(structure)	33.49	180.0	2

Appendix 2. atomic charges on the polyimide oligomer

Table A 2.1.
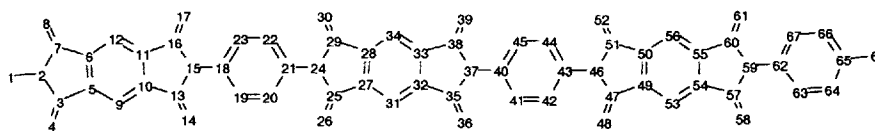
Atom index	Atomic charge/e	Atom index	Atomic charge/e	Atom index	Atomic charge/e
1	0·3033	24	−0·3822	47	1·3659
2	−0·4881	25	1·3666	48	−1·3375
3	1·3652	26	−1·3316	49	0·0246
4	−1·3425	27	−0·0256	50	0·0285
5	0·0302	28	0·0263	51	1·3669
6	0·0200	29	1·3655	52	−1·3306
7	1·3694	30	−1·3345	53	0·0865
8	−1·3432	31	0·0845	54	0·0237
9	0·0847	32	0·0263	55	0·0273
10	0·0249	33	0·0257	56	0·0850
11	0·0223	34	0·0844	57	1·3714
12	0·0879	35	1·3660	58	−1·3363
13	1·3685	36	−1·3368	59	−0·3833
14	−1·3310	37	−0·3843	60	1·3701
15	−0·3818	38	1·3681	61	−1·3275
16	1·3658	39	−1·3354	62	0·3415
17	−1·3348	40	−0·3047	63	−0·1116
18	0·3040	41	−0·0590	64	−0·0431
19	−0·0639	42	−0·0581	65	0·0282
20	−0·0629	43	0·3037	66	−0·0261
21	0·3040	44	−0·0631	67	−0·0620
22	−0·0613	45	−0·0589	68	0·0381
23	−0·0611	46	−0·3828		

References

[1] DEPP, S., and HOWARD, W., 1993, *Sci. Am.*, **268**, 90.
[2] FOSTER, J. S., and FROMMER, J. E., 1988, *Nature*, **333**, 542.
[3] HARA, M., IWAKABE, Y., TOCHIGI, K., SASABE, H., GARITO, A. F., and YAMADA, A., 1990, *Nature*, **344**, 228.
[4] IKEDA, M., OOUMI, M., SHIGENO, M., KITAJIMA, I., SUGINOYA, M., and MUZUTANI, W., 1991, in *Proc. 17th Jpn. Annual Meeting on Liq. Cryst.*, 334.
[5] YONEYA, M., and IWAKABE, Y., 1995, *Liq. Cryst.*, **18**, 45.
[6] CLEAVER, D. J., CALLAWAY, M. J., FORESTER, T., SMITH, W., and TILDESLEY, D. J., 1995, *Mol. Phys.*, **86**, 613.
[7] MAUGUIN, P., 1911, *Bull. Soc. Fr. Min.*, **34**, 71.
[8] BERREMAN, D., 1972, *Phys. Rev. Lett.*, **28**, 1683.
[9] CASTELLANO, J., 1983, *Mol. Cryst. Liq. Cryst.*, **94**, 33.
[10] FUJIWARA, I., ISHIMOTO, C., and SETO, J., 1991, *J. Vac. Sci. Technol. B*, **9**, 1148.
[11] YANG, X., MIN, G., GU, N., LU, Z., and WEI, Y., 1994, *J. Vac. Sci. Technol. B*, **12**, 1981.
[12] AOYAMA, H., YAMAZAKI, Y., MATUURA, N., MADA, N., and KOBAYASHI, S., 1981, *Mol. Cryst. liq. Cryst. Lett.*, **72**, 127.
[13] MURATA, M., UEKITA, M., NAKAJIMA, Y., and SAITOH, K., 1993, *Jpn. J. appl. Phys.*, **32**, L679.

[14] VAN GUNSTEREN, W. F., and BERENDSEN, H. J. C., 1987, *GROMOS Manual*, BIOMOS b.v., Biomolecular Software, Univ. of Groningen, The Netherlands.
[15] PICKEN, S. J., VAN GUNSTEREN, W. F., VAN DUIJNEN, P. T., and DE JEW, W. H., 1989, *Liq. Cryst.*, **6**, 357.
[16] HÄDICKE, E., and BRODE, S., 1993, *Makromol. Chem. Macromol. Symp.*, **65**, 205.
[17] VAN AERLE, N., and TOL, A., 1994, *Macromolecules*, **27**, 6520.
[18] YONEYA, M., and IWAKABE, Y., 1995, *Langmuir*, **11**, 3516.
[19] TAJI, Y., YOKOTA, T., and IWATA, T., 1986, *J. Phys. Soc. Jpn*, **55**, 2676.
[20] LEGGETTER, S., and TILDESLEY, D. J., 1989, *Mol. Phys.*, **68**, 519.
[21] BERENDSEN, H. J. C., POSTMA, J. P. M., VAN GUNSTEREN, W. F., DINOLA, A., and HAAK, J. R., 1984, *J. chem. Phys.*, **81**, 3684.
[22] SANO, M., SASAKI, D. Y., and KUNITAKE, T., 1992, *Science*, **258**, 4
[23] SANO, M., SASAKI, D. Y., YOSHIMURA, S., and KUNITAKE, T., 1994, *Faraday Discuss.*, **98**, 307.
[24] ZANNONI, C., 1979, *The Molecular Physics of Liquid Crystals*, edited by G. R. Luckhurst and G. W. Gray (Academic Press), Chap. 9, p. 191–220.
[25] NEJOH, H., 1991, *Surf. Sci.*, **256**, 94.